Theoretical study of micro-optical structure fabrication based on sample rotation and two-laser-beam interference*

Yizhen Chen(陈宜臻)[1], Xiangxian Wang(王向贤)[1,†], Ru Wang(王茹)[1], Hua Yang(杨华)[1], and Yunping Qi(祁云平)[2]

[1] *School of Science, Lanzhou University of Technology, Lanzhou* 730050, *China*
[2] *College of Physics and Electronic Engineering, Northwest Normal University, Lanzhou* 730070, *China*

(Received 7 November 2016; revised manuscript received 16 December 2016; published online 30 March 2017)

A method for fabricating a micro-optical structure based on sample rotation and two-laser-beam interference is proposed. The rotation process is analyzed using the coordinate transformation in matrix presentation and the theoretical expressions of the optical field distributions corresponding to different sample rotations. By rotating the samples and changing the laser wavelength, various special micro-optical structures can be obtained, such as equally spaced concentric rings and irregular trapezoidal lattices; these structures are demonstrated by simulating the corresponding optical field distributions. The proposed approach may be developed into a low-cost laser interference lithography technology for the fabrication of various micro-optical structures.

Keywords: lithography, micro-optical structure, laser interference, sample rotation

PACS: 42.25.Hz, 81.16.Nd, 42.82.Cr **DOI:** 10.1088/1674-1056/26/5/054203

1. Introduction

Micro-structures have numerous applications, such as in photonic crystals,[1] grating structures,[2] and biosensors.[3] In fact, several micro- and nano-structure fabrication methods have been developed to date, including nano-imprinting, ion-beam lithography (IBL), electron-beam lithography (EBL),[4] x-ray lithography,[5] and atomic force microscope lithography.[6] However, these technologies have a great number of disadvantages in terms of cost, efficiency, and the complexity of the manufacturing process.[7–10] Recently, surface plasmonic lithography[11–13] has been widely studied, as this technique allows fabrication of sub-wavelength structures. In the previous works by the present authors,[14–16] waveguide-mode interference lithography was proposed and presented; this technique can be used to fabricate sub-wavelength gratings with different periods. However, as regards to micro-structure fabrication, including periodic one-dimensional (1D) and two-dimensional (2D) structures, the most commonly used method is laser interference lithography (LIL).[17–22] For example, Jiang *et al.* fabricated 1D and 2D superhydrophobic graphene surfaces by means of two-laser-beam interference;[23] Xuan *et al.* obtained periodic triangle truncated pyramid arrays using an LIL system;[24] and moth-eye structures were fabricated on silicon via six-laser-beam interference lithography by Xu *et al.*[25]

In general, two-laser-beam interference can be used to fabricate simple periodic 1D micro-optical structures. For more complex structures, additional laser beams may be required;[26,27] however, this may complicate the optical devices and increase the operation difficulty. Thus, improvements to the LIL technology and cost performance are also required.[28] Recently, Wang *et al.* fabricated a 2D-lattice optical structure by rotating a sample by 90° after the initial exposure to expose it for a second time.[29] Furthermore, Hassanzadeh *et al.* proposed the fabrication of a large number of interesting microstructures, such as equally spaced concentric rings,[30] using multi-exposure LIL based on the rotation of a Lloyd's mirror interferometer. However, it is difficult to rotate that type of interferometer, and the lithography principles and rotation process involved in the proposed approach have not been widely examined.

In this paper, we propose the use of two-laser-beam interference with two different kinds of photoresist-sample rotation methods for the fabrication of varieties of micro-optical structures with latent application. Based on the coordinate transformation in matrix presentation[31] and the principle of interference of two coherent light beams,[32] a theoretical expression of the optical field distribution is obtained. Hence, via numerical simulation, optical field distributions are simulated to indicate the lithography results of different sample rotation mechanisms. In particular, by simulating multi-exposure with two kinds of laser at different wavelengths, we obtain unequal periodic 2D structures, i.e., a quasi-rectangular lattice and an irregular trapezoid lattice.

*Project supported by the National Natural Science Foundation of China (Grant No. 61505074), the National Basic Research Program of China (Grant No. 2013CBA01703), the HongLiu Young Teachers Training Program Funded Projects of Lanzhou University of Technology, China (Grant No. Q201509), and the National Undergraduate Innovation Training Program of China (Grant No. 201610731030).

†Corresponding author. E-mail: wangxx869@126.com

© 2017 Chinese Physical Society and IOP Publishing Ltd

2. Theoretical analysis

Figure 1 presents a schematic of the proposed micro-optical structure fabrication lithography method, which is based on sample rotation and two-laser-beam interference. Here, a He–Cd laser is assumed as the laser source. The He–Cd laser is typically used in LIL,[17] because it can emit lasers of two different wavelengths, i.e., 325 nm and 442 nm. In addition, the emitted laser can be easily converted from one wavelength to the other, while the beam propagation direction and the position in space remain unchanged. A shutter is used to control the exposure and a beam splitter is used to divide a single laser beam into two coherent parts. The sample is placed on a rotation stage.

It can be assumed that the two coherent light beams that emerge from the beam splitter are plane waves and can be modeled as

$$\boldsymbol{E}_1(\boldsymbol{r}_1,t) = \boldsymbol{E}_{01}\,\mathrm{e}^{\mathrm{i}(\boldsymbol{k}_1\cdot\boldsymbol{r}_1-\omega t+\varphi_1)}, \tag{1}$$

$$\boldsymbol{E}_2(\boldsymbol{r}_2,t) = \boldsymbol{E}_{02}\,\mathrm{e}^{\mathrm{i}(\boldsymbol{k}_2\cdot\boldsymbol{r}_2-\omega t+\varphi_2)}, \tag{2}$$

where $\boldsymbol{E}_{01}$ and $\boldsymbol{E}_{02}$ are the electric field amplitudes, $\boldsymbol{k}_1$ and $\boldsymbol{k}_2$ are the wave vectors, φ_1 and φ_2 are the initial phases, and $\boldsymbol{r}_1$ and $\boldsymbol{r}_2$ are the position vectors of the two beams, respectively. Furthermore, ω is the angular frequency of the waves and t is time. Thus, $\boldsymbol{E}_1(\boldsymbol{r}_1,t)$ and $\boldsymbol{E}_2(\boldsymbol{r}_2,t)$ represent the electric fields of the two beams.

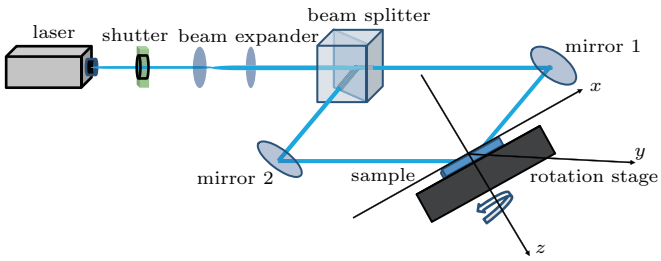


Fig. 1. (color online) Schematic of lithography setup for micro-optical structure fabrication based on sample rotation and two-laser-beam interference.

Assume that the sample is fixed on the x–y plane. Figure 2 shows the propagation of two laser beams emerging from the beam splitter in the x–z plane. Thus, $\boldsymbol{k}_1$ and $\boldsymbol{k}_2$ are perpendicular to the y-axis and the propagating angles (θ) of the two beams relative to the z-axis are identical. We set $\varphi_1 = \varphi_2 = 0$. Thus, the electric fields along the x-axis on the sample surface can be expressed as

$$E_1(x,t) = E_{01}\,\mathrm{e}^{\mathrm{i}(kx\sin\theta-\omega t)}, \tag{3}$$

$$E_2(x,t) = E_{02}\,\mathrm{e}^{\mathrm{i}(kx\sin\theta-\omega t)}, \tag{4}$$

where $k = 2\pi/\lambda$. The superposition of the electric fields of the two individual plane waves gives

$$E(x,t) = E_1(x,t) + E_2(x,t). \tag{5}$$

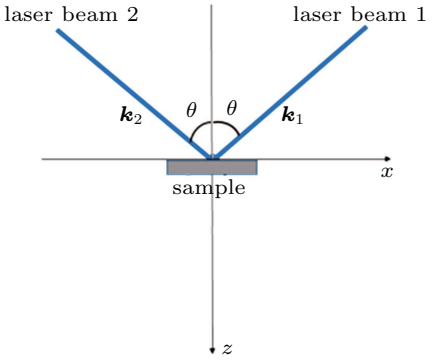


Fig. 2. (color online) Schematic of two-laser-beam interference on the sample surface, where $\boldsymbol{k}_1$ and $\boldsymbol{k}_2$ are the wave vectors and θ is the incidence angle.

The irradiance of the electromagnetic wave is given by $I \propto \boldsymbol{E}^* \cdot \boldsymbol{E}$. Thus, the spatial distribution of the total optical intensity of the two waves interfering on the sample is expressed as

$$I(x) = I_1 + I_2 + 2\sqrt{I_1 I_2}\cos\left(\frac{4\pi\sin\theta}{\lambda}x\right). \tag{6}$$

To simplify the calculation process, we suppose $I_1 = I_2 = 1$; thus, the intensity distribution can be expressed as

$$I(x) = 2\left[1+\cos\left(\frac{4\pi\sin\theta}{\lambda}x\right)\right], \tag{7}$$

with the period of $I(x)$ being

$$\Lambda = \frac{\lambda}{2\sin\theta}. \tag{8}$$

For a sample, two exposure methods are available. In one approach, N exposures are performed with $N-1$ sample rotations. In the other approach, the shutter retains opening and the sample is continuously exposed while being continuously rotated. By utilizing the coordinate transformation in matrix presentation,[31] the optical field distribution after the n-th rotation can be obtained, such that

$$\begin{pmatrix} x_n & y_n & I_n \end{pmatrix} = \begin{pmatrix} x & y & I \end{pmatrix} \begin{pmatrix} \cos\alpha_n & \sin\alpha_n & 0 \\ -\sin\alpha_n & \cos\alpha_n & 0 \\ 0 & 0 & 1 \end{pmatrix}, \tag{9}$$

where $(x_n\ y_n\ I_n)$ is the coordinate matrix of the optical field distribution after the n-th sample rotation and α_n is the rotation angle relative to the first exposure. The initial optical field distribution is represented by $(x\ y\ I)$. For N exposures, the total distribution can be expressed as

$$I(x,y) = \sum_{n=1}^{N} I_n(x,y,\alpha_n). \tag{10}$$

For the second exposure method, we assume that the angular velocity of the rotation is ω_0; hence, the rotation angle can be expressed as a function of time, i.e., $\alpha = \omega_0 t$. Consequently, when the sample is rotating, the field distribution can be expressed as

$$I(x,y,t) = 2\left[1+\cos\left(\frac{4\pi\sin\theta}{\lambda}(x\cos\omega_0 t - y\sin\omega_0 t)\right)\right]. \tag{11}$$

If the total exposure time of the rotation process is T, the total optical field distribution can then be expressed as an integral

$$I_T(x,y) = \int_0^T I(x,y,t)\,\mathrm{d}t. \tag{12}$$

3. Numerical simulation results

Based on the equations obtained above, we employ a numerical simulation to obtain the field distribution for a given rotation/exposure configuration, so as to theoretically demonstrate the corresponding micro-optical structure that could be fabricated in practice. A standing wave optical field distribution is formed via the interference of two coherent lasers according to Eq. (7); thus, a periodic 1D structure can be fabricated utilizing two-laser-beam interference. As an example, we use $\lambda = 325$ nm and $\theta = 10^\circ$ in the simulation. The standing wave optical field distribution simulation results obtained for these parameters are shown in Fig. 3(a). Based on this distribution, a 1D grating with a period of 935.8 nm can be fabricated.

Although the optical field distribution obtained from two coherent lasers is 1D, by exposing the photoresist sample and applying different rotation methods, we can fabricate numerous 2D micro-optical structures. As noted above, one approach is to expose the sample N times with $N-1$ sample rotations. If we rotate the sample by 90° and expose it for a second time with the same exposure dose, a 2D dot array pattern can be recorded on the photoresist sample. This case can be simulated using Eqs. (9) and (10), and the corresponding optical field distribution is shown in Fig. 3(b). A magnified segment of Fig. 3(b) is shown in Fig. 3(c); it is apparent that the dots of the array have a quasi-square shape. Furthermore, if the sample is subjected to three exposures under the same dose with a 60°-rotation after each exposure, a periodic hexagonal structure is obtained (Fig. 4(a)). From Fig. 4(b), a magnification of part of Fig. 4(a), it is apparent that there are six triangles outside this hexagonal structure. However, the optical field intensity of these triangles is very low compared to the hexagon. This difference is demonstrated by the 3D intensity distribution of one period shown in Fig. 4(c).

More interesting and complex structures can be fabricated by exposing and rotating the sample continuously. As an example, we simulate the total optical field distribution for the case in which the sample is continuously rotated with $\alpha = 180^\circ$, $\lambda = 325$ nm, and $\theta = 10^\circ$. An equally spaced concentric ring structure is obtained. Figure 5 shows the simulated results for the 2D and 3D optical field distributions. The intensity distribution along the center line of Fig. 5(a) is shown in Fig. 5(c). From the x-values of the crests and troughs, it can be determined that the loop width is approximately 936 nm, while the radius of the center round is 568 nm. From the graph of the distribution function and the 3D figure of the field distribution (Fig. 5(b)), it is apparent that the optical field of the rings decreases progressively. Further, the field at the center is extremely strong compared to that at the surrounding area.

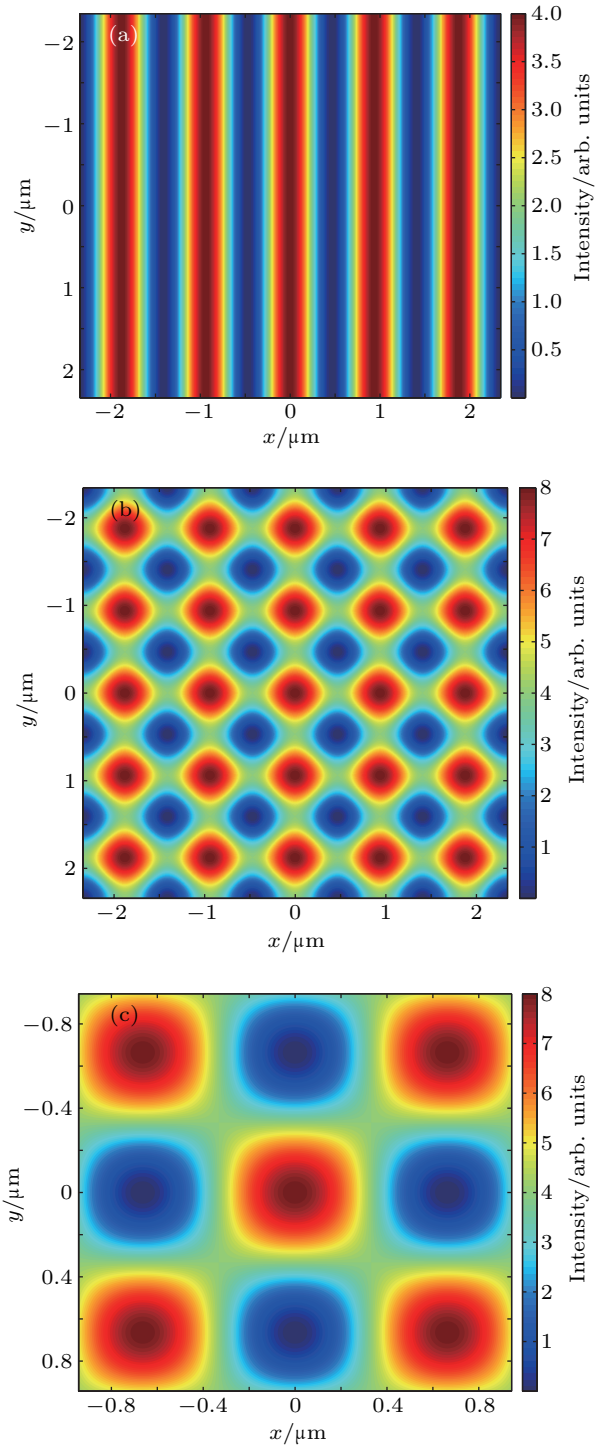


Fig. 3. (color online) (a) 2D optical field distribution for single exposure of two-laser-beam interference. (b) 2D optical field distribution for double exposure and 90°-rotated sample. (c) Magnified segment from panel (b).

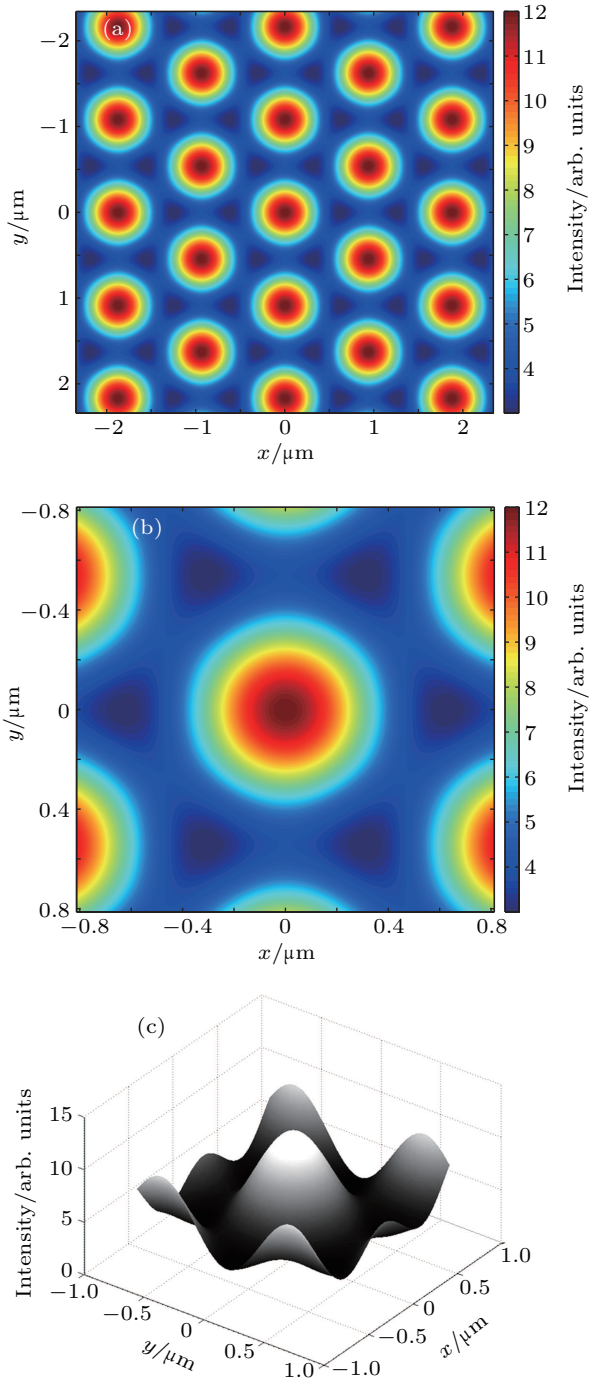


Fig. 4. (color online) (a) 2D optical field distribution for triple exposure, with the sample being rotated by 60° after each exposure. (b) Magnified segment from panel (a). (c) 3D optical field distribution of one period.

As shown in Eq. (8), the period of the standing wave optical field distribution (Λ) is proportional to λ. Therefore, by changing λ, we can fabricate micro-optical structures with vertical Λ values different from the horizontal ones. To achieve this, the sample is first exposed to the 325-nm laser, before being rotated by 90°. The laser wavelength is changed from $\lambda_1 = 325$ nm to $\lambda_2 = 442$ nm, keeping $\theta = 10°$ as before. The sample is then exposed for the second time. The results of this procedure are shown in Fig. 6(a). It is obvious that the field distribution is similar to that shown in Fig. 3(b); however, the dots in Fig. 6(a) have a quasi-rectangular shape, with Λ values of 935.8 nm and 1272.7 nm, whereas the dots in Fig. 3(b) are quasi square.

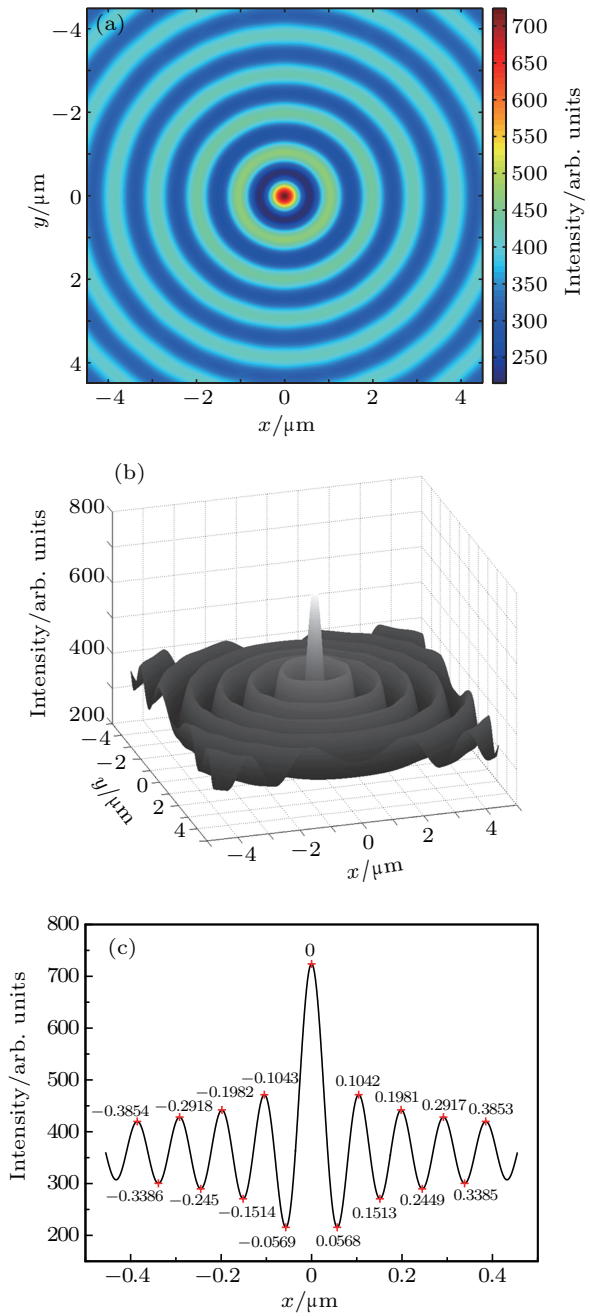


Fig. 5. (color online) (a) 2D optical field distribution for continuous exposure, with the sample being continuously rotated by 180°. (b) 3D optical field distribution. (c) Optical field distribution along the x-axis. The numbers on the crests and troughs are the x-values.

Furthermore, by exposing the sample four times with 45° sample rotations after each exposure ($\lambda_{1-4} = 325$ nm, 442 nm, 325 nm, and 442 nm, respectively), a more interesting structure can be obtained, as shown in Fig. 6(b). The distribution corresponds to an irregular quasi-trapezoidal lattice, but it is centrosymmetric. If we change the rotation and exposure method further, for example, by changing α or λ, additional micro-optical structures can be fabricated.

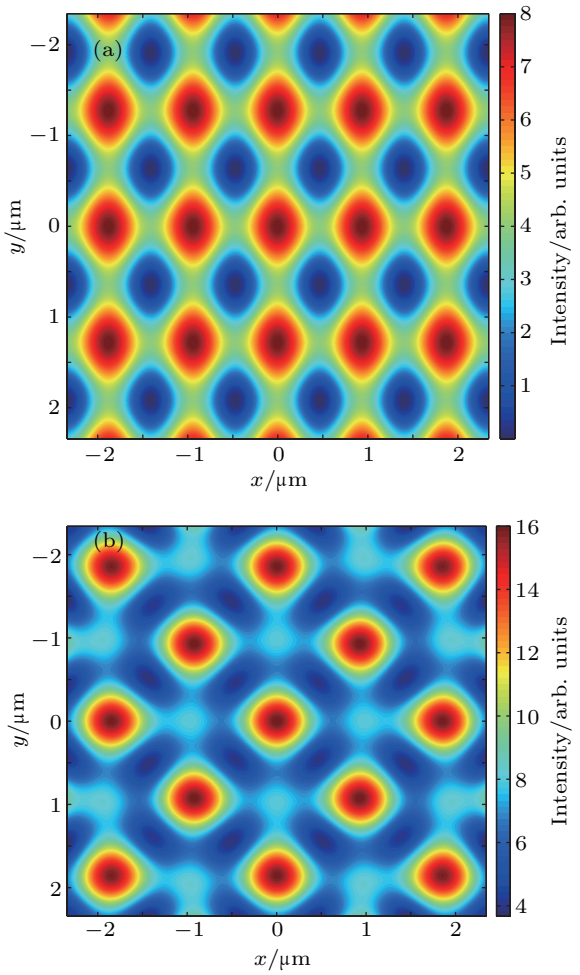


Fig. 6. (color online) (a) 2D optical field distribution for double exposure with different laser wavelengths (325 nm and 442 nm), where the sample rotation angle is 90°. (b) Quadruple exposure, where the wavelength of each exposure is 325 nm, 442 nm, 325 nm, and 442 nm respectively. The sample is rotated by 45° after each exposure.

Various kinds of micro-optical structures can be fabricated using the proposed method, and the structure parameters can be controlled effectively by changing the laser-beam incidence angle and wavelength. The structures discussed above constitute selected examples of the various possibilities only.

4. Conclusion

We have proposed a method of fabricating micro-optical structures by employing sample rotation and two-laser-beam interference. By rotating and exposing a sample in different ways using the suggested interference device, a wide variety of micro-optical structures can be fabricated, such as hexagons and equally spaced concentric rings. By exposing the sample to lasers with different wavelengths, some irregular periodic optical structures can also be obtained. It is hoped that the proposed lithography method can be used for the fabrication of different kinds of micro-optical structures. Further, the microstructures simulated in this study can be applied to numerous micro-optics fields. For example, the 1D grating can be used as a diffraction grating, the periodic hexagonal structure can be employed as a photonic crystal, and the spaced concentric rings can be used as a zone plate. Hence, the proposed technology will have considerable applications in the fields of micro- and nano-optics, because of its simple operation, low cost, and high output.

References

[1] Moon J H, Ford J and Yang S 2006 *Polym. Advan. Echnol.* **17** 83
[2] Shibata S, Che Y, Sugihara O, Okamoto N and Kaino T 2004 *Jpn. J. Appl. Phys.* **43** 2370
[3] Yu F, Li P, Shen H, Mathur S, Lehur C M, Bakowsky U and Mücklichd F 2005 *Biomaterials* **26** 2307
[4] Liu Q, Duan X M and Peng C S 2014 *Novel Optical Technologies for Nanofabrication* (Berlin: Springer-Verlag) pp. 153–178
[5] Heyderman L J, Solak H H, David C, Atkinson D, Cowburn R P and Nolting F 2004 *Appl. Phys. Lett.* **85** 4989
[6] Snow E S and Campbell P M 1994 *Appl. Phys. Lett.* **64** 1932
[7] Harriott L R 2001 *Proc. IEEE* **89** 366
[8] Hinsberg W, Houle F A, Hoffnagle J, Sanchez M, Wallraff G, Morrison M and Frank S 1998 *J. Vac. Sci. Technol.* **16** 3689
[9] Brousseau E B, Dimov S S and Pha D T 2010 *Int. J. Adv. Manuf. Tech.* **47** 161
[10] Hassanzadeh A and Ho Wong K K 2009 *Photonics North 2009*, August 4, 2009, Quebec, Canada, p. 73861
[11] Xie Z H, Yu W X, Wang T S, Zhang H X, Fu Y Q, Liu H, Li F Y, Lu Z W and Sun Q 2011 *Plasmonics* **6** 565
[12] Sreekanth K V and Murukeshan V M 2010 *J. Vac. Sci. Technol.* **28** 128
[13] Yang F, Chen X, Cho E H, Lee C S, Jin P and Guo L J 2015 *Appl. Phys. Express* **8** 062004
[14] Wang R, Wang X X, Yang H and Ye S 2016 *Acta. Phys. Sin.* **65** 094206 (in Chinese)
[15] Wang X X, Zhang D G, Chen Y K, Zhu L F and Yu W H 2013 *Appl. Phys. Lett.* **102** 031103
[16] Wang R, Wang X X, Yang H and Qi Y P 2017 *Chin. Phys. B* **26** 024202
[17] Xie Q, Hong M H, Tan H L, Chen G X, Shi L P and Chong T C 2008 *J. Alloys Compd.* **449** 261
[18] Seo J H, Park J H, Kim S I, Park B J, Ma Z Q, Choi J and Ju B K 2014 *J. Nanosci. Nanotech.* **14** 1521
[19] Yang H F, He H D, Zhao E L, Han J, Hao J B, Qian J G, Tang W and Zhu H 2014 *Laser Phys.* **24** 065901
[20] Kim H, Jung H, Lee D H, Lee K B and Jeon H 2016 *Appl. Opt.* **55** 354
[21] Hang W Q, Dong T G, Wang G, Liu S L, Huang Z M, Miao X J, Lv Q and Qin C J 2015 *Chin. Phys. B* **24** 084205
[22] Siddique R H, Hünig R, Faisal A, Lemmer U and Hölscher H 2015 *Opt. Mater. Express* **5** 996
[23] Jiang H B, Zhang Y L, Han D D, Xia H, Feng J, Chen Q D, Hong Z R and Sun H B 2014 *Adv. Func. Mater.* **24** 4595
[24] Xuan M D, Dai L G, Jia H Q and Chen H 2014 *Optoelectr. Lett.* **10** 51
[25] Xu J, Wang Z B, Zhang Z, Wang D P and Weng Z K 2014 *J. Appl. Phys.* **115** 203101
[26] Lai N D, Liang W P, Lin J H, Hsu C C and Lin C H 2005 *Opt. Express* **13** 9605
[27] Voisiat B, Gedvilas M, Indrišiūnas S and Račiukaitis G 2011 *Phys. Proc.* **12** 116
[28] Cheng L and Lipson R H 2010 *Laser Photon. Rev.* **4** 568
[29] Wang X X, Wang X D, Yang H, Ye S and Yu J L 2015 *J. Func. Mater.* **46** 20132 (in Chinese)
[30] Hassanzadeh A, Mohammadnezhad M and Mittlerb S 2015 *J. Nanophoton.* **9** 093067
[31] Boas M L 2006 *Mathematical Methods in the Physics Science* (3nd Edn.) (Chichester: John Wiley and Sons) pp. 126–130
[32] Born M and Wolf E 1999 *Principles of Optics* (7nd Edn.) (England: Cambridge University Press) pp. 287–289